Magnetic Resonance in Medicine 44:277–282 (2000)

Recording of the Event-Related Potentials During Functional MRI at 3.0 Tesla Field Strength

F. Kruggel,* C.J. Wiggins, C.S. Herrmann, and D.Y. von Cramon

The feasibility of recording event-related potentials (ERP) during functional MRI (fMRI) scanning was studied. Using an alternating checkerboard stimulus in a blocked presentation, visually evoked potentials were obtained with their expected configuration and latencies. A clustered echoplanar imaging protocol was applied to observe the hemodynamic response due to the visual stimulus interleaved with measuring ERPs. Influences of the electrode/amplifier set up on MRI scanning and the scanning process on the recording of electrophysiological signals are reported and discussed. Artifacts overlaid on the electrophysiological recordings were corrected by *post hoc* filtering methods presented here. Implications and limitations of conducting combined ERP/fMRI experiments using higher-level cognitive stimuli are discussed. Magn Reson Med 44: 277–282, 2000. © 2000 Wiley-Liss, Inc.

Key words: functional magnetic resonance imaging; event-related potentials; cardio-ballistic effect; filtering; multi-modal imaging

Measurable correlates of neuronal activation in the brain include electromagnetic fields (here measured by event-related potentials (ERP)) and the hemodynamic response (here measured by functional magnetic resonance imaging (fMRI) of the vascular system). The first effect is a direct consequence of the electrical activity of neurons, and thus features the same millisecond timescale as the underlying cognitive process, while the second is only indirectly linked to the energy consumption of the neuronal population, and takes place on a timescale which is on the order of seconds. However, recent developments in experimental techniques and data analysis have shown that hemodynamic responses are indeed modulated by the experimental stimulation and carry information about the underlying processes at least on a 100 ms timescale (1–4). The localization of an activation by ERP source analysis suffers from poor spatial resolution and the theoretical problem of providing only inexact solutions. Here, fMRI is better able to localize brain activations at a high spatial resolution.

It is obvious that a combination of both techniques is a very attractive aim in neuroscience, and a number of research groups have taken up the challenge. To the best of our knowledge, all of these studies were performed as separate experiments (i.e., ERP and fMRI recordings at different times), and results were registered and combined by data processing (e.g., (5–7)). One of the criticisms of this approach is that it is impossible to control whether a subject performs in the same manner in both experiments. However, a combined measurement (i.e., recording ERPs during fMRI scanning) reveals a number of delicate technical problems: gradients applied during fMRI scanning induce voltages which are much higher than the brain's response, and thus interrupt electroencephalogram (EEG) acquisition; much similar artifacts are due to cable movement in the field; in addition, electrodes and leads of the EEG setup can also possibly interact with the fMRI scanning process.

A number of research groups have worked on the technical details of the problems of recording an EEG in the magnetic field (8–13). One of the main problems encountered was the occurrence of a pulse-synchronous artifact, which reached amplitudes of 100–500 μV and thus hid the real EEG signal. Head movements induced by heart action lead to small movements of the electrodes and cables in the magnetic field, and thus induce a voltage in the wires.

Unfortunately, the amplitude of this artifact is expected to increase with the field strength of the scanner (14). We report on our experiences of recording EEG in a 3.0 T magnetic field. A careful experimental set up and *post hoc* signal correction procedures allow the reliable recording of visually evoked potentials (VEP), and a modified echoplanar imaging (EPI) protocol made it possible to simultaneously measure the blood–oxygen level dependent (BOLD) effect elicited by the visual stimulation.

MATERIALS AND METHODS

Five healthy persons took part in this study (3 female, 2 male, mean age 23.6 years, range 21–27 years). All subjects had previous experience as test persons in EEG and fMRI studies. They received a nominal compensation for their effort. All subjects gave informed consent in accordance with guidelines set by the Max-Planck-Institute.

Subject Setup

Conventional plastic-coated Ag/AgCl electrodes with iron-free copper leads 60 cm long were fixed on the subject's scalp by a stretchable plastic cap. Electrodes were mounted at positions Fz, F3, F4, C3, C4, P3, P4, O1 and O2 of the international 10/20 system. Fz was used as reference. Cables were twisted pairwise and led through a flexible silicon tube to the EEG amplifier located above the subject's head along the body axis in the scanner tunnel. In order to minimize movements, the subject's head was restrained using cushions. Cables and amplifier were fixed to the gantry by tape and weighed down by rice bags. Subjects wore mirror glasses in order to perceive the visual stimulation.

Stimulation

To elicit visual evoked potentials, a black/white checkerboard pattern of 16 × 16 patches (full field visual angle

Max-Planck-Institute of Cognitive Neuroscience Stephanstraße 1, 04103 Leipzig, Germany.

*Correspondence to: Frithjof Kruggel, Max-Planck-Institute of Cognitive Neuroscience, Stephanstraße 1, D-04103 Leipzig, Germany.
E-mail: kruggel@cns.mpg.de

Received 10 December 1999; revised 22 March 2000; accepted 23 March 2000.

11.5 degrees, 42 arc min per pattern) was inverted in intervals of 550 ms (a trial) (15). The ERTS package (Berisoft GmbH, Frankfurt, Germany) was used for stimulus display programming. The stimulation pattern was projected onto a screen in the scanner tunnel from an LCD projector located outside the scanner room. In experimental condition A, 256 trials were recorded *without* fMRI scanning. Condition B was designed as a blocked-fMRI experiment of 16 repetitions. Each block consisted of 16 sec checkboard stimulation, followed by a 16 sec display of a fixation point (corresponding to a total of 310 trials). Both conditions were run twice in each subject. A single trigger pulse was sent from the MR console to the stimulation PC to start an experimental block.

EEG Recording

A commercially available MR-compatible system (Schwarzer, Munich, Germany) was used for EEG recording. The battery-powered amplifier located in the scanner tunnel was connected via a 20 m fiber optic link to a standard PC in the MR console room equipped with a digital signal processor (DSP) board. The DSP board received trigger input from the stimulation PC which was recorded with the biosignals. The amplification factor of the system was 10000 $\times$, with a bandwidth of 0.073-70 Hz. Biosignals were sampled at 250 Hz using an unipolar recording with Fz as reference. Collected data were analyzed offline (see below).

fMRI Scanning

Functional imaging was performed using a Bruker Medspec 30/100 3.0T MR system. A bird cage quadrature coil was used. An in-house EPI implementation allowed the acquisition of the slices to be collected together at the beginning or end of the TR time, thus providing long pauses during which no MR signals were being recorded for the collection of the EEG data. Sequence parameters were: TE 30 ms, TR 1333 ms between successive acquisition of the same slice. Three slices were acquired with thickness 5 mm with 2 mm gap, 19.2 cm FOV, 64 $\times$ 64 matrix with 100 kHz sampling. The time period during which the images were acquired was 200 ms, leaving a 1133 ms period for MR relaxation and EEG acquisition. The three slices were centered along the sagittal direction of the calcarine fissure.

EEG Data Evaluation

Recorded EEG data were processed in a series of steps as described below. Samples from the signal of electrode channel c at time point t are denoted $y(c, t)$, and C corresponds to the number of electrodes, T to the number of time points. *Slow-frequency components* of the signal were removed using a Hamming-weighted high-pass filter with a cut-off frequency of 0.8 Hz. In data from condition B, *artifacts from MR gradient pulses* were detected in the summed signal $y'(t) = \Sigma_{c=1}^{C} |y(c, t)|$. If the slope of this signal exceeded a threshold $\Delta y'/\Delta t > 25$ μV/ms, an interval of the following 200 ms was marked for exclusion. The *cardio-ballistic artifact* was corrected using a procedure similar to the one described by Allen et al. (14). First, cardiac cycles were detected. The EEG was averaged across all electrodes using the equation $y'(t) = [\Sigma_{c=1}^{C} y(c, t)]/C$, and low-pass filtered using a cut-off frequency of 6 Hz. The autocorrelation of this signal was computed in a window of 5 sec. The first peak (except $t = 0$) was stored as the length of this cardiac cycle, and the window moved by the length of this cycle. For each channel c and each cycle, a section of the artifact model $y'(t)$ was adapted to the original signal $y(c, t)$ by varying an amplitude factor a, an offset o, and a (small) temporal shift t_0:

$$\{a, o, t_0\} = \arg \min_{a,o,t_0} \left[\sum (y(c, t) - a * (y'(t + t_0) + o))^2 \right] \quad [1]$$

where the summation included all time points of a given cycle. The adapted artifact model was subtracted from the signal, which was low-pass filtered using a cut-off frequency of 30 Hz to yield the corrected EEG. Finally, trials were averaged within the same condition. In condition B, marked intervals were excluded.

fMRI Data Evaluation

Subject movements were corrected in 2D (two translational and one rotational parameter) within and between both scans in condition B (16). *Baseline filtering* was achieved by estimating the baseline using low-pass filtering in the temporal domain (cut-off 0.05 Hz) and subtraction of the result from the data (17). *System and physiological noise* were partially removed by low-pass filtering in the temporal domain (cut-off 0.2 Hz) (17). *Functional activation* was detected by voxelwise univariate regression analysis using a box-car waveform shifted by 5 sec to match the lag of the hemodynamic response. The F-scores obtained were corrected for the effective degrees of freedom by analyzing the temporal auto-correlation (18). *Assignment of significance* was achieved by conversion of the F-scores into z-scores, thresholding the z-score map by eight, and assessment of the activated regions for their significance on the basis of their spatial extent (19). For graphical display, significantly activated brain areas were color-coded and overlaid onto T_1-weighted anatomical scans obtained at the same positions as the functional data. In addition, z-score maps were registered with a T_1-weighted high-resolution MR dataset of the same subject and transformed into Talairach space, in order to determine the coordinates of the fMRI activation centers.

Dipole Fitting

In order to demonstrate the close coupling of BOLD response and EEG activity, sources of the visual ERPs were localized using the ASA software package (ANT Software, Enschede, The Netherlands) on the basis of a realistically shaped three-shell boundary element model of the human brain and skull.

RESULTS

Correction of the Cardioballistic Artifact

As reported previously (e.g., (8,11,13,14)) the biosignal recorded on the scalp was overlaid by large artifacts when

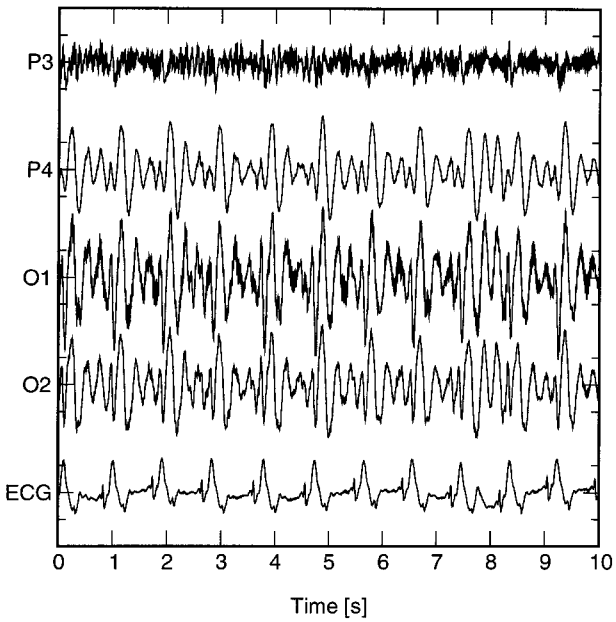

FIG. 1. Signal recorded *inside* the scanner at sample scalp positions and corresponding ECG (tick marks on EEG traces, ± 200 μV; on ECG trace, ± 1 mV). This biosignal is about five times larger than recordings outside the scanner.

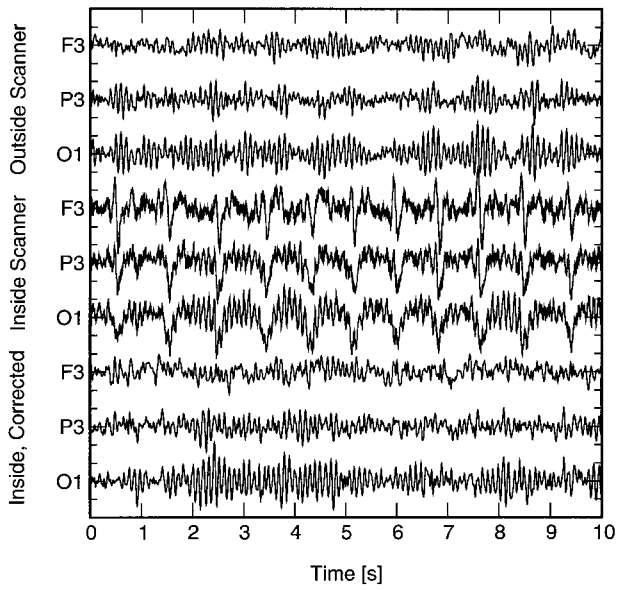

FIG. 2. Spontaneous EEG *outside* the scanner (top, tick marks, ± 50 μV); *inside* the scanner (middle, tick marks, ± 200 μV); and EEG corrected for the cardioballistic artifact (below, tick marks, ± 50 μV). Trace labels correspond to electrode locations.

the subject was within the main magnet field of the scanner (see Fig. 1).

The amount of this artifact differed by electrode site (frontal more than occipital), in the distance between electrode and reference position and between subjects. It often reached 500 μV, hiding the EEG signal. In experiments with a watermelon phantom we found that even small vibrations (e.g., tapping on the gantry, acoustically-induced vibrations) induced a measurable signal. We concluded that movements of any kind are the major source of artifacts overlaid on the EEG obtained inside the scanner. Careful subject fixation, as described above, reduced the artifact level considerably. However, even when fixing subjects as much as tolerable, the artifact dominated the recorded signal, so the application of the *post hoc* correction algorithm was necessary in all recordings. An example result is shown in Fig. 2.

The top three rows correspond to EEG channels F3, P3, and O1, recorded outside the scanner; the middle three rows correspond to a recording from the same channels, but inside the scanner. Note that the scale was reduced by a factor of four. The bottom rows show the corrected signal. Most likely, small head movements induced by each pulse wave induce this artifact, which has been called the "cardioballistic effect".

ERP Experiment

The VEP experiment was run twice in each subject, both for condition A (without fMRI scanning) and condition B (with fMRI scanning). Typically configured, reproducible VEPs in the form of a P2/N3 complex were found in all subjects and all runs. The grand average is shown in Fig. 3 where the dotted line corresponds to averages from condition A, and the solid line to condition B. Note that the results from condition B were slightly worse.

Latencies of P2 and N3 components in single subjects were determined and compared with published data (recorded outside of a magnetic field). No differences between conditions and reference data were found using a Kruskal-Wallis test (see Table 1).

fMRI Experiment

In all subjects and both runs of condition B, the typical BOLD activation from visual stimulation was detected. No

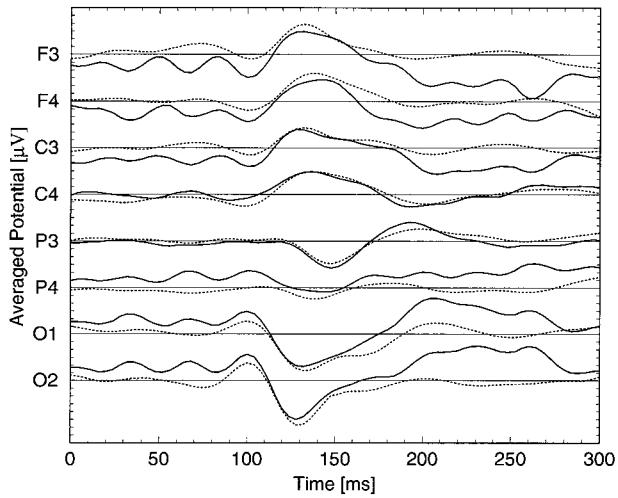

FIG. 3. Grand average (n = 5) for the VEP experimental condition A (dotted line, without fMRI scanning); and condition B (with fMRI scanning). Electrode Fz was used as reference.

Table 1
Mean and Variance of Latencies (in ms) for P2 and N3 Components of the VEP, Recorded Under Both Conditions, in Comparison With Reference Values

Condition	P2	N3
Condition A (without scanning)	100.0 ± 8.5	131.4 ± 7.1
Condition B (with scanning)	101.0 ± 4.4	129.4 ± 4.9
Reference 1 (20)	98.1 ± 5.3	128.3 ± 13.2
Reference 2 (13)	106 (91–120)	155 (133–173)

No significant difference between latencies was found in a Kruskal-Wallis test between condition A, B, and reference 1. Values cited as reference 2 correspond to results from an experiment similar to condition A.

interference of electrodes (e.g., artifacts due to susceptibility differences) or shielding effects of the wires were noticed. An example result of a single subject is shown in Fig. 4 along with the VEP recorded from the corresponding electrodes O1 and O2.

Dipole Fitting

Dipoles were fitted to the N3 component of a single subject in a time window between 100–128 ms. Two initial dipoles were placed in the occipital cortex at the center of the fMRI activations, corresponding to Talairach coordinates (−8, −100, 0) and (8, 100, 0). Figure 5 shows the two occipital dipoles in a top view and a side view. The variance of the ERP data is explained to 97% by these dipoles. This very good fit is also considered as a quality measure for the ERP component.

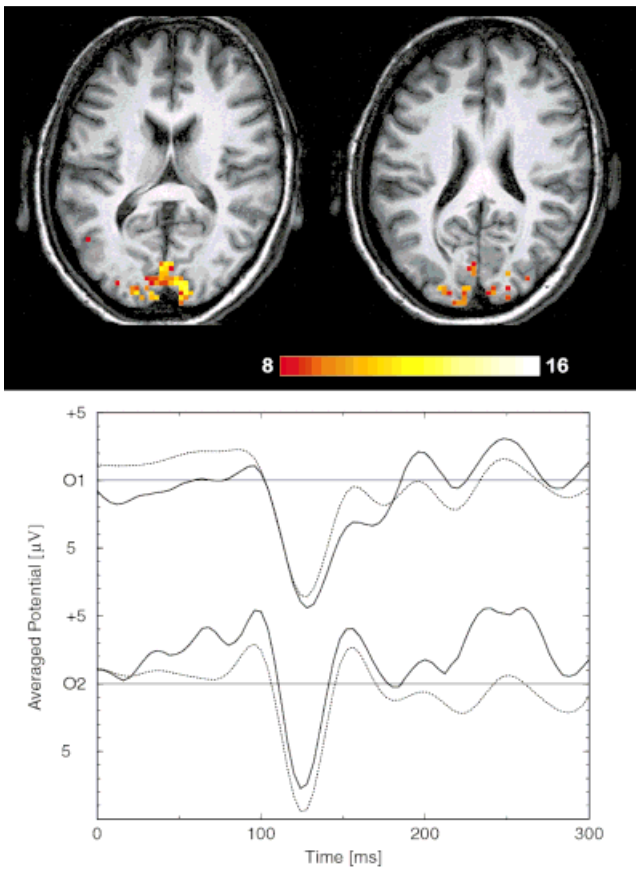

FIG. 4. Example results from a single subject: BOLD activation (top) shown as a z-score color map overlaid onto the corresponding anatomical slices and visually evoked potential (below). Here, the dotted line corresponds to condition A (without fMRI scanning); the solid line to condition B (with fMRI scanning).

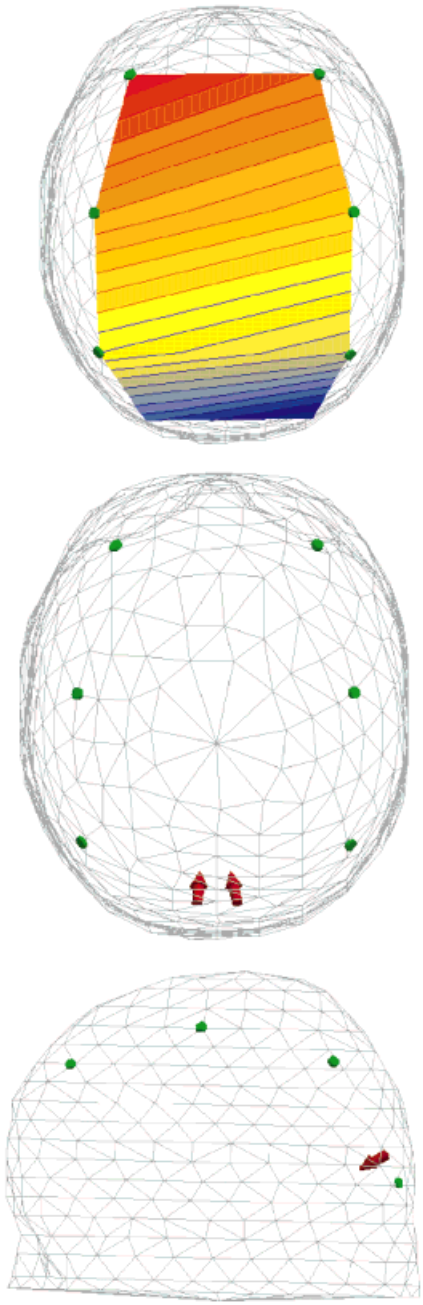

FIG. 5. Top, potential distribution of the measured ERP (top view). Below, both occipital dipoles which explain the ERP data to 97% (top and side view).

DISCUSSION

The feasibility of recording ERPs during fMRI scanning was demonstrated by recording VEPs with the expected

configuration while measuring the BOLD response at the striate cortex. Subjects did not report any adverse effects of a combined measurement. No noticeable influences of the electrode setup on fMRI scanning were found in the data obtained.

The EEG recorded during fMRI scanning was disturbed by MR gradient activation (for which time intervals were excluded) and overlaid by movement-induced artifacts. As previously reported (e.g., (13,14)), it was necessary to implement a procedure to correct for the pulse-synchronous portion of these artifacts. Müri et al. (13) used an electrocardiogram-locked stimulus presentation in order to generate an artifact model. This approach requires that cardiac cycles be relatively constant during an experimental condition, and that the stimulus presentation be short (i.e., less than a cycle). Both conditions are unsuitable for performing cognitive experiments because stimulus presentation often lasts for a couple of seconds, and also because we found heart rate variations typically of 20%. We consider that an advantage of using an adaptive procedure in this study was that our VEP component latencies better correspond with published data outside the scanner, and exhibit a lower variance (see Table 1). Allen et al. (14) proposed an adaptive approach which is based on a 10 sec history to correct and display the EEG for spike detection. Because we were not interested in the ongoing EEG, we could afford to apply a post hoc procedure which is more elaborate and more costly in terms of computational demands: our artifact model was generated trace- and epoch-wise from a small temporal window around a given epoch. This model was shifted and scaled in time and amplitude in order to optimally fit this epoch. Subtraction of the fitted model nicely recovered the EEG (see Fig. 2).

The experiment reported here is considered to be a first step toward the study of higher-level cognitive processes by combined ERP/fMRI measurements. When weighing arguments for combined vs. separate measurements, the following issues need to be raised:

- Only a small number (nine) of electrodes were used in this study, while conventional ERP experiments are run with 64 or 128 electrodes. Using the higher number of electrodes is necessary to cover a larger portion of the scalp (and the brain underneath), and to achieve a better spatial resolution of the recorded biosignals. However, when using a high electrode and cable density, influences on fMRI acquisition are more likely.
- Artifacts overlaid on the EEG will always lead to a lower signal-to-noise ratio in combined measurements. As a consequence, the quality of obtained ERPs is lower in comparison with separate measurements, and minute differences between ERP components from different experimental conditions might be lost. Due to discomfort in the scanner, an experiment duration of more than 40–50 min is hardly feasible, thus imposing an upper limit for the number of trials.
- It was impossible to recover the EEG during MR gradient activity, and these periods were simply excluded from evaluation. Thus, fMRI acquisition was clustered to leave a "silent period" for EEG acquisition. Because the lag of the hemodynamic response is in the order of 4–6 sec, both the electrophysiological and the hemodynamic response from the same event may be observed. However, simultaneous recordings impose a compromise between the fMRI and EEG acquisition time within a TR period, thus limiting the number of fMRI slices.
- In this simple experiment, a blocked design with a single condition (on/off) was chosen in order to obtain a sufficient signal-to-noise ratio for both modalities. Because a "rest state" is not defined, cognitive experiments usually employ differences between multiple sets of stimulus conditions to make inferences about the relation between recorded signals and brain processes. While the experimental design has matured for separate fMRI and ERP experiments, limitations as discussed above for a combined measurement impose severe constraints for the design of cognitive experiments. Conventional single-trial designs for fMRI do not include enough trials to ensure a good signal-to-noise ratio for obtaining a reasonable quality of ERPs. However, recent advances in experimental design and data analysis, such as the fast, temporally jittered presentation of single trials (21), may offer a solution for this problem.

At this time, it appears too early to make any conclusion about the usefulness of combined ERP/fMRI measurements for cognitive studies. But even within limits as discussed above, a lot of prospects are open for performing combined experiments using higher-level cognitive tasks. Especially appealing is the possibility of observing complementary responses from the same stimulation event on a single subject level, in order to better understand physiological processes underlying brain activation and the functional organization of the brain.

REFERENCES

1. Buckner RL. Event-Related fMRI and the hemodynamic response. Hum Brain Mapp 1998;6:373–377.
2. Clark VP, Maisog JM, Haxby JV. FMRI study of face perception and memory using random stimulus sequences. J Neurophysiol 1998;79:3257–3265.
3. Richter W, Andersen P, Georgopoulos AP, Kim SG. Sequential activity in human motor areas during a delayed cued finger movement task studied by time-resolved fMRI. Neuro Report 1997;8:1257–1261.
4. Kruggel F, von Cramon DY. Modeling the Hemodynamic response in single-trial functional MRI experiments. Magn Reson Med 1999;42: 787–797.
5. Martinez A, Anllo-Vento L, Sereno MI, Frank LR, Buxton RB, Dubowitz D, Wong EC, Hinrichs H, Heinze HJ, Hillyard SA. Involvement of striate and visual cortical areas in spatial attention. Nat Neurosci 1999;2:364–369.
6. Opitz B, Mecklinger A, von Cramon DY, Kruggel F. Combining electrophysiological and hemodynamic measures of the auditory oddball. Psychophysiology 1999;36:142–147.
7. Woldorff MG, Tempelmann C, Fell J, Tegeler C, Gaschler-Markefski B, Hermann H, Heinze HJ, Scheich H. Lateralized auditory spatial perception and the contralaterality of cortical processing processing as studied with fMRI and MEG. Hum Brain Mapp 1999;7:49–66.
8. Chiappa KH, Huang-Hellinger F, Jenkins BG, Hill RA. EEG during MR imaging: differentiation of movement artifact from paroxysmal cortical activity. Neurology 1995;45:1942–1943.
9. Huang-Hellinger F, Breiter HC, McCormack G, Cohen MS, Kwong KK, Sutton JP, Savoy RL, Weisskopf RM, Davis TL, Baker JR, Belliveau JW, Rosen BR. Simultaneous functional magnetic resonance imaging and electrophysiological recording. Hum Brain Mapp 1995;3:13–23.

10. Ives RJ, Warach S, Schmitt F, Edelmann RR, Schmoer DL. Monitoring the patient's EEG during echo planar MRI. Electroenceph Clin Neurophysiol 1993;87:417–420.
11. Krakow K, Allen PJ, Polizzi G, Lemieux L, Fish DR. The amplitude and distribution of EEG pulse artifact in the MR scanner: its effect on the detection of EEG events. In: Proceedings of the 6th Meeting of the ISMRM, Sydney, 1998. p 1494.
12. Lemieux L, Allen PJ, Franconi F, Symms MR, Fish DR. Recording of EEG during fMRI experiments: patient safety. Magn Reson Med 1997; 38:943–952.
13. Müri RM, Felbinger J, Rösler KM, Jung B, Hess CW, Boesch C. Recording of electrical brain activity in a magnetic resonance environment: distorting effects of the static magnetic field. Magn Reson Med 1998; 39:18–22.
14. Allen PJ, Polizzi G, Krakow K, Fish DR, Lemieux L. Identification of EEG events in the MR scanner: the problem of the pulse artifact and a method for its subtraction. Neuro Image 1998;8:229–239.
15. Celesia CG, Brigell MG. Recommended standards for pattern electroretinograms and visual evoked potentials. Electroenceph Clin Neurophysiol 1999;Suppl. 52:53–67.
16. Friston KJ, Williams S, Howard R, Frackowiak RSJ, Turner R. Movement-related effects in fMRI time series. Magn Reson Med 1996;35:346–355.
17. Kruggel F, von Cramon DY, Descombes X. Comparison of filtering methods for fMRI datasets. Neuro Image 1999;10:530–543.
18. Worsley KJ, Friston KJ. Analysis of fMRI time-series revisited—again. Neuro Image 1996;2:173–181.
19. Friston KJ, Worsley KJ, Frackowiak RSJ, Mazziotta JC, Evans AC. Assessing the significance of focal activations using their spatial extent. Hum Brain Mapp 1994;1:210–220.
20. Jörg J, Hielscher H. Evozierte Potentiale in Klinik und Praxis. Heidelberg: Springer; 1989.
21. Burock MA, Buckner RL, Woldorff MG, Rosen BR, Dale AM. Randomized eventrelated experimental designs allow for extremly rapid presentation rates using functional MRI. Neuroreport 1998;9:3735–3739.